

# Angular Signatures of Dark Matter in the Diffuse Gamma Ray Spectrum

Dan Hooper and Pasquale D. Serpico

*Particle Astrophysics Center, Fermi National Accelerator Laboratory, Batavia, IL 60510-0500, USA*

Dark matter annihilating in our Galaxy's halo and elsewhere in the universe is expected to generate a diffuse flux of gamma rays, potentially observable with next generation satellite-based experiments, such as GLAST. In this article, we study the signatures of dark matter in the angular distribution of this radiation. Pertaining to the extragalactic contribution, we discuss the effect of the motion of the solar system with respect to the cosmological rest frame, and anisotropies due to the structure of our local universe. For the gamma ray flux from dark matter in our own Galactic halo, we discuss the effects of the offset position of the solar system, the Compton-Getting effect, the asphericity of the Milky Way halo, and the signatures of nearby substructure. We explore the prospects for the detection of these features by the GLAST satellite and find that, if  $\sim 10\%$  or more of the diffuse gamma ray background observed by EGRET is the result of dark matter annihilations, then GLAST should be sensitive to anisotropies down to the 0.1% level. Such precision would be sufficient to detect many, if not all, of the signatures discussed in this paper.

PACS numbers: 95.35.+d, 95.85.Pw, 98.70.Vc

FERMILAB-PUB-07-038-A

## I. INTRODUCTION

The spectrum of gamma rays generated in dark matter annihilations has the potential to serve as a valuable tool in exploring the physical and astrophysical properties of dark matter. As the dark matter annihilation rate scales with the square of the density, one would naively expect the brightest sources of gamma rays to be nearby and high-density objects, such as the Galactic Center [1], dwarf spheroidal galaxies [2], or other local dark matter structures [3].

It is not necessarily the case, however, that these sources are the easiest targets to detect the flux of dark matter annihilation radiation. In particular, the distributions of dark matter in the Galactic Center, dwarf spheroidals and other such regions are not well known. Although N-body simulations predict that dark matter halos should contain high density cusps in their centers [4, 5], mechanisms have been proposed which would modify this prediction. This is particularly true in the innermost regions of these halos, where additional phenomena involving baryons or central black holes may be relevant [6]. As the rate of dark matter annihilations in these halos depend critically on the density in their innermost centers, it is extremely difficult to reliably estimate the brightness of dark matter annihilation radiation from this class of regions.

Astrophysical sources of gamma rays can also provide a formidable background for dark matter searches from local, high density sources. In particular, the Galactic Center has been found by HESS and other gamma ray telescopes to contain a bright source of very high energy radiation [7]. The presence of this source poses a very serious challenge to future dark matter searches in the Galactic Center [8].

With these issues in mind, it is difficult to assess the expected signal and corresponding background expected from annihilating dark matter in nearby, high density regions, even within the context of a well-defined particle physics model. Moreover, even if such a source were observed, one might be concerned whether it could be reliably identified as dark matter radiation, rather than as another class of astrophysical object. Only with a high precision measurement of the gamma ray spectrum, ideally including the detection of mono-energetic lines, could point sources of dark matter annihilation radiation be conclusively identified.

An alternative target for indirect dark matter searches is the diffuse, or unresolved, contribution to the gamma ray spectrum [9–12]. According to high resolution cold dark matter simulations and other theoretical arguments, large virialized dark matter halos are formed through the repeated mergers of smaller halos formed at earlier times. As a result of this process, dark matter structures are expected to consist of large numbers of microhalos or clumps. Given the fact that the annihilation signal scales with the square of the dark matter density, the presence of substructure can result in a huge enhancement in the gamma ray flux with respect to the naive estimate for a smooth distribution [13]. For a simple argument justifying this conclusion, see Appendix A.

The gamma ray signal from dark matter halos (including our own Galaxy) depends crucially on the fraction of microhalos that survive the hierarchical merging process, as well as the density profiles, spatial distribution and mass spectrum of those which survive. The lack of knowledge of the dark matter power spectrum on very small scales, the difficulty involved in calculating gravitational clustering in the deep

non-linear regime, and uncertainties in the effects of the tidal stripping of clumps by both dark matter and baryonic structures conspire to make current estimates of the average annihilation rate uncertain by orders of magnitude, independently of unknowns regarding the particle identity of the dark matter candidate. At present, it is even unclear whether the diffuse dark matter signal should be dominated by our Galactic halo or by the extragalactic component. Furthermore, even if our Galaxy's halo dominates the diffuse gamma ray spectrum, it is not clear from which direction, and to what extent, the emission from clumped dark matter will dominate the overall flux from dark matter annihilations.

A lot of attention has been given in the literature to studying the spectrum of gamma rays in order to identify signatures of dark matter (for a recent example, see Ref. [14]). Although this has the potential to be a powerful diagnostic tool, it will be challenging to clearly separate a dark matter signal from alternative astrophysical sources unless very precise measurements are performed with a larger number of events and/or over a large energy range. This is especially true in the case of diffuse radiation and in scenarios where dark matter annihilations only provide a subleading contribution to the total gamma ray flux.

In this paper, we mainly focus our attention to the complementary information provided by the angular patterns in the diffuse radiation generated in dark matter annihilations. In Sec. II, we provide a simple parametrization of the Galactic and extragalactic diffuse dark matter fluxes and discuss under which circumstances each of these components dominate. Secondly, we summarize the key signatures and distinctive features of the dark matter diffuse gamma ray radiation if dominated by the extragalactic (Sec. III) or Galactic contribution (Sec. IV). We also discuss the prospects for the detection of these signatures by the forthcoming generation of instruments, in particular the GLAST satellite (Sec. V). We summarize our conclusions in Sec. VI.

## II. GALACTIC VS. EXTRAGALACTIC DOMINANCE

In this section, we compare the relative importance of the Galactic and extragalactic contributions to the diffuse gamma ray emission. Depending on which of these dominates, different signatures are expected in future gamma ray observations.

We begin by computing the galactic halo emission. This is made by two contributions: one from the smooth halo and another by the fraction of the density retained in clumps. We closely follow the approach of Ref. [15], although we retain the angular and energy dependence and use a slightly different notation. The differential flux of photons (in units of photons per area per time per steradian per energy) from dark matter annihilations with a smooth distribution can be written as

$$I_{\text{sm}}(E, \psi) = f_{\gamma}(E) \Pi \int_{\text{l.o.s.}} ds \frac{\rho_{\text{sm}}^2[r(s, \psi)]}{4\pi}, \quad (1)$$

where

$$r(s, \psi) = \sqrt{r_{\odot}^2 + s^2 - 2 r_{\odot} s \cos \psi}, \quad (2)$$

$\psi$  is the angle between the direction in the sky and the Galactic Center,  $r_{\odot} \approx 8.0$  kpc is the solar distance from the Galactic Center, and  $s$  the distance from the Sun along the line-of-sight (l.o.s.). Particle physics enters via the term

$$f_{\gamma}(E) \Pi \equiv f_{\gamma}(E) \frac{\langle \sigma_{\text{ann}} v \rangle}{2 m_{\chi}^2}, \quad (3)$$

where  $m_{\chi}$  is the WIMP mass, the factor  $1/2$  enters since we assume that dark matter constitutes its own anti-particle, and  $\langle \sigma_{\text{ann}} v \rangle$  is the annihilation cross section. The function  $f_{\gamma}(E)$  is the photon differential energy spectrum per annihilation (with units of  $E^{-1}$ ). This spectrum per annihilation is largely the result of the fragmentation and hadronization of the WIMP's annihilation products.

A general class of smooth halo distributions can be fitted as

$$\rho_{\text{sm}}(r) = \rho_{\odot} \left( \frac{r_{\odot}}{r} \right)^{\gamma} \left( \frac{r_{\odot}^{\alpha} + a^{\alpha}}{r^{\alpha} + a^{\alpha}} \right)^{\epsilon}, \quad (4)$$

where  $\rho_{\odot}$  is the dark matter density at the solar distance from the Galactic Center, and  $a$  is a characteristic scale radius below which the profile scales as  $r^{-\gamma}$ . Two of the most well known profiles have been

proposed by Navarro, Frenk and White (NFW) [4], with  $\gamma = 1, \alpha = 1, \epsilon = 2$  and Moore *et al.* [5] with  $\gamma = 3/2, \alpha = 1, \epsilon = 3/2$ . A cored isothermal profile is recovered in the case of  $\gamma = 0, \alpha = 2, \epsilon = 1$  [16].

These profiles differ primarily in the central region. Since here we are focusing on the Galactic diffuse emission rather than that from the Galactic Center, our choice of halo profile is not critical. The uncertainties which are introduced through the choice of profile (within a factor  $\sim 2$ ) are negligible for our discussion. For definiteness, we shall adopt an NFW profile with  $\rho_{\text{sm}}(r_{\odot}) = 0.3 \text{ GeV/cm}^3$  and  $a = 45 \text{ kpc}$ .

The clumpy signal can be written instead as

$$I_{\text{cl}}(E, \psi) = \frac{f_{\gamma}(E)}{4\pi} \int_{\text{l.o.s.}} ds \int dM \int dR n_{\text{cl}}[r(s, \psi), M, R] \Gamma_{\text{cl}}(M, R), \quad (5)$$

where  $M$  is the mass of the microhalos,  $R$  their size, and  $n_{\text{cl}}[r(s, \psi), M, R]$  is the number density distribution (differential with respect to the  $M$  and  $R$ ) of microhalos as a function of  $M$ ,  $R$  and the distance from the Galactic Center,  $r$ . The exact range over which the  $M$  and  $R$  integrals are carried out depends indirectly on the cosmology and the particle physics model which is considered.  $\Gamma_{\text{cl}}(M, R)$  is the annihilation rate from a single microhalo, and can be written as

$$\Gamma_{\text{cl}}(M, R) = \int_V d^3\mathbf{x} \frac{\langle \sigma_{\text{ann}} v \rangle}{2m_{\chi}^2} \rho_{\text{cl}}^2(\mathbf{x}) \equiv \bar{\rho}_{\text{cl}}^2 V S \Pi = \bar{\rho}_{\text{cl}} M S \Pi, \quad (6)$$

where  $\bar{\rho}_{\text{cl}}$  is the average density of the clump,  $M$  and  $V$  its mass and volume, respectively, and  $S$  is a geometrical factor that depends of the density profile of the clump, such that  $S = 1$  for an homogeneous distribution. If we *assume*

$$\int dM \int dR n_{\text{cl}}[r(s, \psi), M, R] M = \xi \rho_{\text{sm}}[r(s, \psi)], \quad (7)$$

then we can rewrite Eq. (5) as

$$I_{\text{cl}}(E, \psi) = f_{\gamma}(E) \Pi S \xi \bar{\rho}_{\text{cl}} \int_{\text{l.o.s.}} ds \frac{\rho_{\text{sm}}[r(s, \psi)]}{4\pi}. \quad (8)$$

In Eq. (7), we introduce the reasonable hypothesis that the number distribution of clumps traces the smooth distribution of the halo. This has been confirmed, at least to some degree, in simulations (for a discussion of this point, see Ref. [15]). This approximation is most reliable at large galactic radii and for large mass substructures. For low mass clumps and small galactic radii, tidal interactions with stars are likely to destroy such objects [17]. In our own Galaxy, for example, most of the mass in microhalos at the solar circle will have been highly stripped, forming cold streams of tidal debris.

To account for interactions with bulge stars, we conservatively discard the predictions of annihilation rates in the inner regions  $r \lesssim 3 \text{ kpc}$  ( $|\psi| \lesssim 20^\circ$ ). The effect of interactions with disk stars will only effect the over all annihilation rate by a factor of  $\mathcal{O}(1)$ , which is subleading with respect to other unknowns. We briefly comment on this effect, when relevant, in the following.

Combining the smooth and clumpy components, the total galactic signal can be written as

$$I_{\text{gal}}(E, \psi) \equiv [I_{\text{sm}} + I_{\text{cl}}](E, \psi) = \frac{1}{4\pi} f_{\gamma}(E) \Pi \int_{\text{l.o.s.}} ds \rho_{\text{sm}}[r(s, \psi)] \times (\rho_{\text{sm}}[r(s, \psi)] + S \xi \bar{\rho}_{\text{cl}}). \quad (9)$$

Plugging in typical numbers from simulations ( $S \approx 5$  and  $\bar{\rho}_{\text{cl}} \approx 2 \times 10^{-22} \text{ g cm}^{-3}$  [15]), one infers that even small degrees of substructure (as low as  $\xi \sim 10^{-3}$ ) are sufficient to cause the clumpy contribution to dominate over the smooth component everywhere but in the innermost region of the galaxy. Notice that within simplifying but reasonable hypotheses, the clumpy contribution only depends on a single effective parameter, the product  $S \xi \bar{\rho}_{\text{cl}}$ . For definiteness, we shall use in the following the (free) parameter  $\zeta$ , defined as  $\zeta \equiv \xi \times [S/5] \times [\bar{\rho}_{\text{cl}}/(2 \times 10^{-22} \text{ g cm}^{-3})]$ . The parameters  $\xi$  and  $\zeta$  are, therefore, equal when the other factors assume their fiducial values.

On the other hand, the extragalactic contribution to the diffuse gamma ray spectrum is given by [10]

$$I_{\text{ex}}(E) = \frac{c}{4\pi} \Pi \int_0^\infty dz \frac{\rho_{\text{dm}}^2(z)}{H(z)(1+z)^3} f_{\gamma}[E(1+z)] e^{-\tau(E, z)}, \quad (10)$$

where the Hubble function,  $H(z)$ , is related to the present Hubble expansion rate,  $H_0$ , through the matter and the cosmological constant energy density,  $H(z) = H_0 \sqrt{\Omega_M(1+z)^3 + \Omega_\Lambda}$ . The factor  $e^{-\tau(E, z)}$

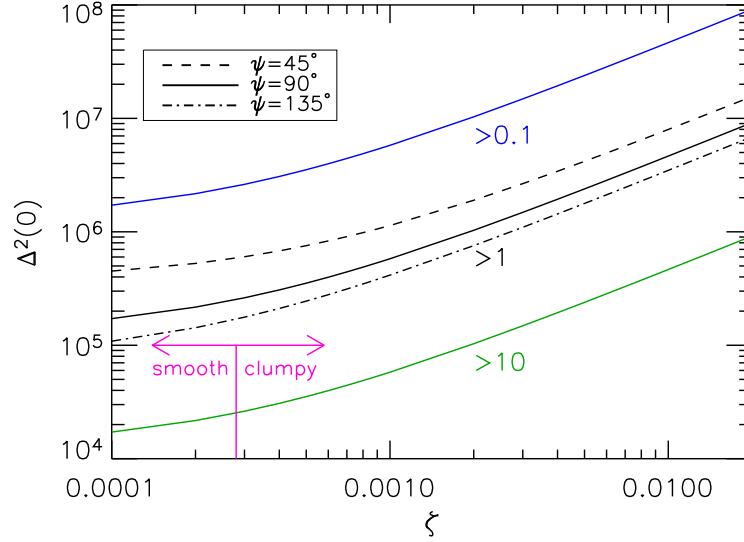


FIG. 1: The contours  $F_{\text{gal}}/F_{\text{ex}} = 0.1, 1, 10$  in the direction orthogonal to the Galactic plane ( $\psi = \pi/2$ ) in the  $\zeta - \Delta^2(0)$  plane, as well as the contour  $F_{\text{gal}}/F_{\text{ex}} = 1$  for three values of  $\psi$ . In the lower-right part of the plot, the Galactic radiation dominates the dark matter contribution to the diffuse flux. To the right of the purple vertical line, the contribution from clumps dominates over the smooth halo term at  $\psi = \pi/2$ .

accounts for the finite optical depth,  $\tau$ , of the universe to high energy gamma rays due largely to scattering with the cosmic infrared background. The clumpiness of the dark matter is usually taken into account by writing

$$\rho_{\text{dm}}^2(z) \equiv \left( \frac{\rho_{\text{dm},0}}{\rho_{c,0}} \right)^2 \rho_{c,0}^2 (1+z)^6 \Delta^2(z) = \Omega_{\text{dm}}^2 \left( \frac{3H_0^2}{8\pi G_N} \right)^2 (1+z)^6 \Delta^2(z), \quad (11)$$

where the so-called enhancement factor,  $\Delta^2(z)$ , can be parameterized approximately as (see, for example, Ref. [10])

$$\Delta^2(z) = \frac{\Delta^2(0)}{(1+z)^3}, \quad (12)$$

where  $\Delta^2(0)$ , at least for  $z \lesssim 3$ , has only a weak dependence from  $z$ . We will neglect any  $z$  dependence in  $\Delta^2(0)$ . According to simulations,  $\Delta^2(0)$  can have values ranging from  $10^4$  to  $10^8$  [18]. All together,

$$I_{\text{ex}}(E) = \frac{c}{4\pi} \Pi \Omega_{\text{dm}}^2 \rho_{c,0}^2 \Delta^2(0) \int_0^\infty dz \frac{f_\gamma[E(1+z)] e^{-\tau(E,z)}}{H_0 \sqrt{\Omega_M(1+z)^3 + \Omega_\Lambda}}. \quad (13)$$

The relative weight of the Galactic and extragalactic contributions has only a weak dependence on the spectral shape,  $f_\gamma$ . In the following, we shall consider the integral quantity,  $F_i(\psi) \equiv \Pi^{-1} \int dE I_i(\psi)$ . We also adopt, for definiteness,  $m_\chi = 100$  GeV whenever not specified otherwise.

In Fig. 1, we show in the  $\zeta - \Delta^2(0)$  plane the three contours  $F_{\text{gal}}/F_{\text{ex}} = 0.1, 1, 10$  in the direction orthogonal to the Galactic plane ( $\psi = \pi/2$ ), where the astrophysical contribution to the diffuse flux is minimized. For the  $F_{\text{gal}}/F_{\text{ex}} = 1$  case, we also show results for two other values of  $\psi$  ( $\pi/4$  and  $3\pi/4$ ). In the lower-right region of the plot, the Galactic radiation dominates the dark matter annihilation contribution to the diffuse flux (the absolute flux depends on the factor  $\Pi$ ). To the right of the purple vertical line, the contribution from clumps dominates over the smooth halo term at  $\psi = \pi/2$ .

Although very rough, the simple model sketched above is useful for understanding qualitatively some features, as illustrated by the following example. In Ref. [19], the claim is made that a dominant fraction of the high energy diffuse gamma ray spectrum measured by EGRET [20, 21] is consistent with being due to  $m_\chi \sim 500$  GeV annihilating neutralinos, without violating existing constraints. Ref. [22], in contrast, concludes that it is hardly conceivable that dark matter annihilation could be a main constituent of the

extragalactic background without exceeding the observed gamma ray flux from the Galactic Center, at least if the density profile of the Milky Way is not very different from that found in other galaxies. We note here that the two statements are equally valid within the presently allowed parameter space, although they assume very different priors. The enhancement factor considered in Ref. [19] is around  $\Delta^2(0) \sim 10^7$  (where the extragalactic flux is likely to dominate for any reasonable value of  $\zeta$ ), while in Ref. [22], values of  $\Delta^2(0) \sim 10^4 - 10^5$  are assumed (for which the galactic flux dominates over the extragalactic one for any reasonable value of  $\zeta$ ). Note that already a boost of  $10^2 - 10^3$  in the enhancement factor would bring the expectation of Ref. [22] for the extragalactic contribution within an order of magnitude of the EGRET flux, similar to the findings of Ref. [19]. Although, as correctly noted in Ref. [22], the parameters that we call here  $\zeta$  and  $\Delta^2(0)$  are to some extent correlated, it is plausible that a “large”  $\zeta$  value might not affect significantly the Galactic Center signal, but only the Galactic diffuse signal, due to the effects of tidal disruption, for example. Namely, the Galactic Center flux, which has the highest uncertainty due to the unknown extrapolation of the smooth halo profile, has probably no significant contribution from the clumpy fraction of the halo.

### III. DISTINCTIVE PATTERNS OF A DOMINANTLY EXTRAGALACTIC CONTRIBUTION

#### A. Cosmological Compton-Getting Effect

An observer in motion with velocity,  $\mathbf{u}$ , relative to the coordinate system in which the distribution of gamma rays is isotropic will measure an anisotropic flux. If gamma ray sources are, on average, at rest with respect to the cosmological frame, the magnitude and direction of the velocity,  $\mathbf{u}$ , of the solar system can be deduced from the detection of the dipole anisotropy of the CMB,  $u = 369 \pm 2$  km/s in the direction  $(l, b) = (263.86^\circ, 48.24^\circ)$  [23]. Since  $u \equiv |\mathbf{u}| \ll 1$ , the anisotropy is dominated by the lowest moment, *i.e.* its dipole moment. The Galactic analogue of this effect was first noticed as a diagnostic tool for cosmic rays by Compton and Getting [24].

The amplitude of this anisotropy can be derived from the Lorentz invariance of the the phase space distribution function,  $f$ , in the frame of the observer and of the emitters (see, for example, Ref. [25]). A first order expansion allows one to deduce the shape of the differential intensity. The intensity in the moving frame can be written as

$$I'(E, \mathbf{n}) \simeq I(E) \left[ 1 + \left( 2 - \frac{d \ln I}{d \ln E} \right) \mathbf{u} \cdot \mathbf{n} \right], \quad (14)$$

where in the above formula  $\mathbf{n}$  is the generic direction and the identification of the energy in the two frames  $E = E'$  has been made consistently with the first order result. The function,  $I(E)$ , is the number of particles per unit solid angle and unit energy that pass per unit of time through an area perpendicular to the direction of observation, and it is related to the phase space density,  $f$ , by  $I(E) \simeq E^2 f(E)$ . Thus a dipole anisotropy is expected with an amplitude given by

$$A \equiv \frac{I_{\max} - I_{\min}}{I_{\max} + I_{\min}} = \left( 2 - \frac{d \ln I}{d \ln E} \right) u, \quad (15)$$

which is independent of energy as long as the energy spectrum does not change, *i.e.* when it can be approximated by a single power-law. Taking into account the observed spectrum of diffuse gamma rays  $I(E) \propto E^{-2.1}$  [20], one infers  $A = (2 + 2.1) u \simeq 0.5\%$ . Note that the Earth’s motion with respect to the Sun induces a subleading (8%) modulation in the vector  $\mathbf{u}$ . Unfortunately, this is not characteristic of a dark matter signal, but would be shared by any cosmic distribution of sources. Yet, its detection (or limits on its amplitude) would allow one to constrain the fraction of the diffuse gamma ray background emitted by cosmological sources [25], which would translate into a conservative constraint on the product,  $f_\gamma \times \Pi \times \Delta^2(0)$ .

#### B. Intrinsic Anisotropies

The distribution of the dark matter in the present day universe is highly structured. As a result, intrinsic anisotropies should be present in the diffuse gamma ray background from dark matter annihilations. Recently, it has been proposed that one could use the peculiar anisotropy at small-scales to probe dark

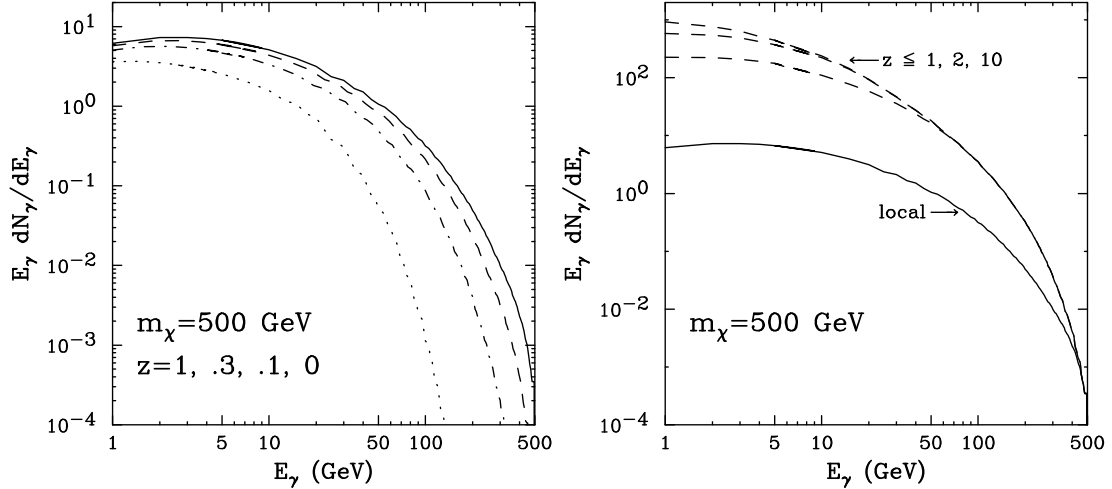


FIG. 2: Left: The shape of the gamma ray spectrum from dark matter annihilations from four redshifts (0, 0.1, 0.3 and 1.0), including the effects of redshift energy losses and absorption with the cosmic infrared background. In the right frame, we compare the spectral shape of gamma rays from local dark matter annihilations (solid) to that from sources integrated out to a redshift of 1, 2 and 10 (from bottom-to-top, dashed). We have assumed that  $\Delta^2(0)$  is roughly constant over this range of redshifts. In each frame, a 500 GeV WIMP annihilating to  $W^+W^-$  was considered. The cosmic infrared background spectrum found in Ref. [28] was adopted.

matter [26]. Provided that dark matter contributes in a relevant way to the diffuse flux, this signature has promising chances to be detected by GLAST. This interesting conclusion was recently extended in Ref. [27], which notes that most of the anisotropy pattern at relatively large angular scales is due to nearby large scale structures. This means that one can use the whole information of a real large-scale structure catalog, going far beyond mere statistical predictions. Although some degree of correlation with large scale structures is also expected in astrophysical models for the production of gamma rays, a key distinctive feature (besides the spectral shape) is the quadratic correlation with overdensity expected for dark matter annihilation radiation.

Additionally, very high energy gamma rays from high redshift sources can be absorbed through interactions with infrared background photons,  $\gamma + \gamma_{\text{IRB}} \rightarrow e^+e^-$ . This effectively shrinks the observable horizon for gamma rays with energies higher than  $\mathcal{O}(0.1-1)$  TeV. In the left frame of Fig. 2 we plot the spectral shape of gamma rays produced in dark matter annihilations at four redshifts,  $z = 0, 0.1, 0.3$  and 1.0. Here, we have considered a 500 GeV WIMP annihilating to  $W^+W^-$ . In the right frame, we show the shape of the gamma ray spectrum from dark matter annihilations integrated out to a redshift of  $z = 1, 2$  and 10 (from bottom-to-top, dashed), compared to the harder spectral shape emitted at redshift zero, e.g. from a local source (solid). Here, we have assumed that  $\Delta^2(0)$  is constant in this range of redshifts. In each frame, we have adopted the model of the cosmic infrared background spectrum found in Ref. [28].

For high energy photons, pair production energy loss is sufficiently effective such that the anisotropies depend almost entirely on the structure of dark matter in the local universe (within several hundred Mpc or so). In this case, cosmological uncertainties, the energy spectrum of the dark matter signal (in dark matter models), the redshift evolution of the sources, etc., each play subleading roles. Additionally, while the “local” anisotropic flux is almost unchanged, at increasingly high energies, the far isotropic component is cut away more and more. The relative anisotropy is higher the greater the energy cut. Together with the many modes available ( $2l + 1$  for each multipole coefficient,  $C_l$ ) and the absence of the cosmic variance limitation, this compensates, to some extent, for the lower statistics available in the  $E \gtrsim 0.1$  TeV range. Of course, the strength of this technique depends critically on the mass of the WIMP being considered. See Ref. [27] for further details.

#### IV. DISTINCTIVE PATTERNS OF A DOMINANTLY GALACTIC CONTRIBUTION

It is well known that the angular distribution of gamma radiation from dark matter annihilation in the Galactic halo has potentially interesting signatures (see, for example, the seminal paper, Ref. [29]). In the following, we summarize the basic features expected.

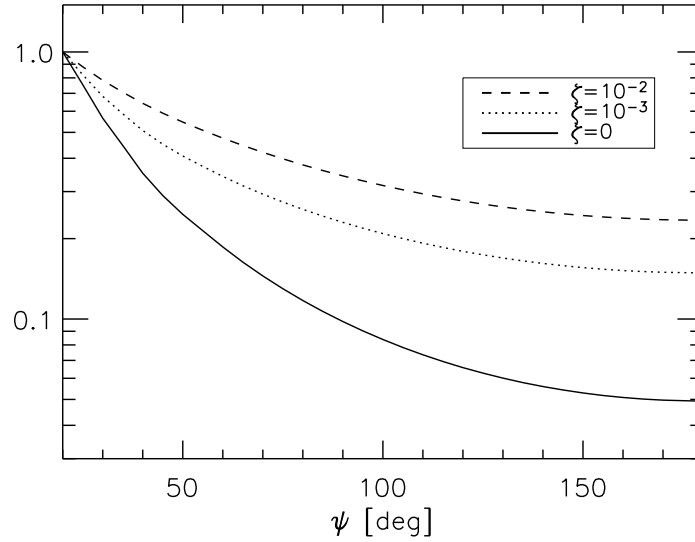


FIG. 3: The angular profile of the Galactic emission of gamma's from dark matter annihilation for three values of the clumpiness parameter,  $\zeta$ . The curves have been normalized to 1 at  $\psi = 20^\circ$ . The region  $\psi < 20^\circ$  is not shown, since it is affected by large uncertainties (see text for discussion).

#### A. Offset Position of the Sun

In the limit of exact spherical symmetry of the dark matter halo, an observer placed in the center of the distribution would observe an isotropic annihilation signal. This follows trivially from Eq. (2) in the limit  $r_\odot \rightarrow 0$ . However, the Sun is offset with respect to the center of the Galactic halo. This induces a peculiar angular dependence, with a maximum toward the inner Galaxy and a minimum toward the antagalactic Center. We show this in Fig. 3 for three values of  $\zeta$ . In the limit of spherically symmetric halo, this is independent of the azimuthal angle,  $\phi$ , around the Sun-Galactic Center line. This signature is fairly robust in two limits:

- A) When  $\zeta \lesssim 0.0002$  (and  $\Delta^2(0) \lesssim 10^5$ ) and the angular distribution is dominated by the smooth halo (bottom curve in Fig. 3). For example, the ratio of the flux at  $\psi = 45^\circ$  to the flux at  $\psi = 135^\circ$  is about 5.
- B) When  $\zeta \gtrsim 0.0005$  (and  $\Delta^2(0) \lesssim \text{few} \times 10^5$ ) and the angular distribution is dominated by the clumpy halo (top curve in Fig 3). In the limit of negligible tidal disruption ( $P(r) \simeq 1$ ), the ratio of the flux at  $\psi = 45^\circ$  to the flux at  $\psi = 135^\circ$  is of about 2.2.

Note that the two models considered in Ref. [30] correspond to these two extreme situations. It is, however, important to point out that, in the most realistic case of the variable  $P(r)$  and a dominant clumpy contribution, this anisotropy feature is likely to be partially suppressed [17], and paradoxically one may end with an almost isotropic flux despite the offset position of the Sun.

Furthermore, since clumps orbiting in the Galactic disk are more easily disrupted than those with “polar” orbits, a slightly lower emission should result from the disk plane than from the vertical one [17, 31]. That is, the flux would acquire a modulation in  $\phi$  even in the limit of a spherical dark matter halo. Although an interesting feature, we note that it may be difficult to observe this effect, which is suppressed when masking the low-latitude Galactic diffuse emission, which is likely dominated by astrophysical sources.

#### B. Compton-Getting Effect (Proper Motion of the Sun in the Halo)

A second signature, which to the best of our knowledge is discussed in detail here for the first time in relation to dark matter, is purely kinematic. Unlike the disk of our Galaxy, which is supported against

radial collapse by its angular momentum, the dark halo is supported by random velocities which serves as a collisionless pressure. It is expected that the velocities of dark matter particles were isotropized at the time of the formation of the Galaxy in the so-called process of “violent relaxation” [32], and should retain this distribution as long as no relevant interaction with the collisional baryonic gas intervenes (for a more extended discussion, see Ref. [33]). Thus, the halo should not have an appreciable rotation as a whole. If it were rotating, it would be flattened similarly to the disk. For our Galaxy, observational constraints imply that the halo is almost spherical, with differences between the axes of the best-fit spheroid not larger than  $\sim 10 - 20\%$  [34, 35].

The Galactic disk rotates around the center of the Galactic halo with a velocity of about 220 km/s at the solar galactocentric distance (see *e.g.* Ref. [35] and references therein). Analogously to the previously discussed extragalactic case, this would be manifest as a halo Doppler effect. In this Galactic case, the dipole points in the direction of motion of the rotation of the Galaxy, and with an amplitude of about 0.3% [see Eq. (15)]. Note that in the case of a Galactic astrophysical (non-dark matter) origin of the diffuse gamma ray flux, this effect is not present, since the disk is on average co-moving with the Sun, with typical proper velocities much smaller than the bulk one. This signature is, therefore, specific to dark matter, unlike its extragalactic counterpart described in Sec. III A.

### C. Asphericity of the Halo

Thus far, we have implicitly assumed that the dark matter distribution in the halo has a spherical symmetry. Simulations of the halo structure, however, show some departure from the spherical symmetry, and typical dark matter halos are actually spheriodals with a moderate eccentricity.

The impact of this effect on the annihilation flux was discussed in detail in Ref. [29], and we shall not repeat here that analysis. Qualitatively, the anisotropy in the emission may be comparable to the effect of the offset position of the Sun. However the symmetry axes of the halo are unknown. Thus the magnitude, the exact angular dependence and the direction of this anisotropy are unknown, making identification of this effect challenging.

### D. Proper Anisotropy Due to Clumpiness

As in the case of extragalactic emission, the typical parameters of the clumps are reflected as peculiar angular signatures of the annihilation signal in the sky. In contrast to the signatures considered above, this is most important at small scales, unless a few clumps happen to be very near us (and in the case that they are resolved, it may also be possible to detect their proper motion [36]). While a highly clumpy and steady emission may be a spectacular signature of dark matter annihilation, it is difficult to obtain model-independent predictions on the expected angular power spectrum, since the physical processes determining the result are highly non-linear and entangled (such as mergers, tidal disruptions, etc.). Furthermore, the observer-related “galactic variance” may greatly change the expected signal. Some attention has previously been given to this kind of signature within the context of superheavy dark matter decays connected with the ultra-high energy cosmic rays [37].

## V. PROSPECTS FOR GLAST

Regarding the detectability of dark matter annihilations through the various angular signatures described in this paper, we shall limit our discussion to the GLAST satellite detector [38]. Although the current generation of atmospheric Cerenkov telescopes, including HESS [39], MAGIC [40] and VERITAS [41], are highly sensitive to very high energy gamma rays, possibly including dark matter radiation, they are best suited for studying point sources rather than diffuse emission. The GLAST experiment is currently scheduled to begin its mission on October 7, 2007.

The flux of gamma rays due to dark matter annihilation is at present unknown. To the best of our knowledge, it may account for a significant or even dominant fraction of the diffuse gamma ray background, especially at the highest measured energies [19]. A residual, isotropic radiation usually interpreted as extragalactic gamma ray background has been measured by GLAST’s predecessor, EGRET [20]. The



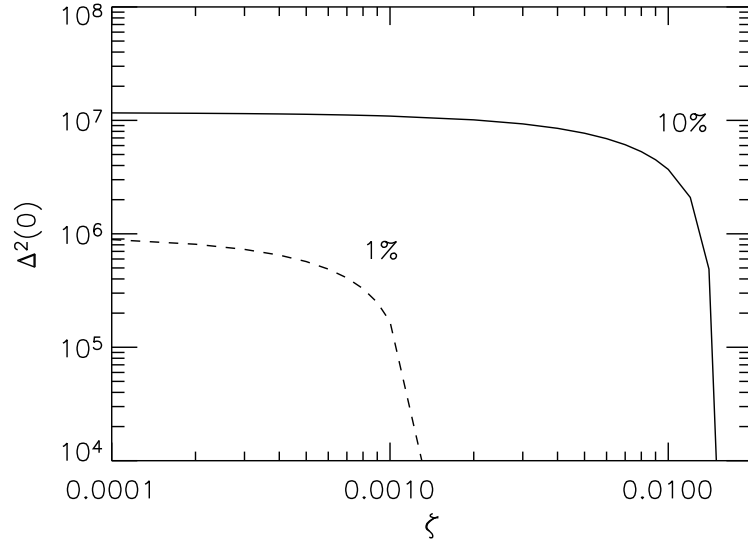


FIG. 4: Contours in the  $\zeta - \Delta^2(0)$  plane (see Sec. II) illustrating the fraction of the diffuse flux observed by EGRET (above 1 GeV) which is the product of dark matter annihilations. Above and to the right of the solid line, more than 10% of this flux is produced by dark matter. Above and to the right of the dashed line, dark matter generates 1% or more of this flux. Here, we have used a 100 GeV WIMP with a  $3 \times 10^{-26} \text{ cm}^3/\text{s}$  annihilation cross section. The Galactic flux being considered here is at a direction perpendicular to the Galactic plane.

intensity of this spectrum can be fit by [20] (see also Ref. [21])

$$I_{\text{cosmic}}(E_\gamma) = (7.32 \pm 0.34) \times 10^{-6} \left( \frac{E_\gamma}{0.451 \text{ GeV}} \right)^{-2.10 \pm 0.03} \text{ cm}^{-2} \text{ s}^{-1} \text{ sr}^{-1} \text{ GeV}^{-1}, \quad (16)$$

over an energy range from  $E_\gamma \sim 10 \text{ MeV}$  to  $E_\gamma \sim 100 \text{ GeV}$ . The number of events collected above an energy,  $E_\gamma$ , can be written as

$$N_\gamma = t \cdot \Omega_{\text{fov}} \cdot \int_{E_\gamma}^{\infty} dE A_{\text{eff}}(E) I_{\text{cosmic}}(E), \quad (17)$$

where  $\Omega_{\text{fov}}$  is the solid angle of the field-of-view,  $A_{\text{eff}}(E)$  is the effective collecting area of the instrument (averaged over its field-of-view), and  $t$  is the time observed. The LAT detector on board GLAST features  $A_{\text{eff}}(E) \simeq 10^4 \text{ cm}^2$  for  $E \gtrsim 1 \text{ GeV}$  (and  $A_{\text{eff}}(E) > 4000 \text{ cm}^2$  for  $E \gtrsim 0.1 \text{ GeV}$ ),  $\Omega_{\text{fov}} \simeq 2.4 \text{ sr}$ , and excellent hadronic background rejection capabilities [38]. Even when considering realistic fractions of data to be rejected from the use of mask cuts or a non-ideal duty-cycle, at least  $\mathcal{O}(10^6)$  diffuse photons per year should be measurable, given the background flux measured by EGRET. Considering up to a decade of operation, it is clear that as long as dark matter is responsible for a significant fraction of the flux of Eq. (16), say at least 10-15%, GLAST should be sensitive to anisotropies down to the 0.1% level. This precision should be sufficient to detect the tiniest of the signatures considered in this paper. For illustrative purposes, in Fig. 4 we show the regions in the parameter space where the DM flux amounts to more than 10% or 1% of the EGRET flux given by Eq. (16), assuming typical parameters for the DM candidate, and fluxes integrated above 1 GeV. In the region above the solid line the collected statistics would allow one to detect all the signatures discussed in this article. Most of these signatures should be detectable in the region above the dashed line. Interestingly, in the lower left corner of the parameter space where the DM flux is subdominant, the signatures of the smooth halo signal should be prominent. Since the offset position of the Sun implies anisotropies of  $\mathcal{O}(100\%)$ , even in this range the prospects for the detection of DM signatures are more promising than what one would naively deduce from Fig. 4.

Of course, a major obstacle in detecting such features are astrophysical foregrounds, which can make the identification of the above signatures difficult (the same is true, of course, when considering spectral energy features). There are, fortunately, a number of qualitative properties of dark matter signals which may help in distinguishing them from astrophysical emissions. The strategy to reveal peculiar extragalactic

features has been discussed elsewhere [27, 42] and we shall not repeat it here. We want only to stress that, qualitatively, after bright sources are removed, a significant cross-correlation with large scale structure catalogs or the CMB dipole direction would provide important diagnostics and a tool for background rejection.

In case of dominance of the Galactic halo emission, it is important to note that: (i) The offset position of the Sun produces a  $\psi$ -dependent asymmetry. (ii) The Doppler effect due to our motion in the halo produces a dipolar asymmetry in the azimuthal angle,  $\phi$ , which for a fixed  $\psi$  identifies the direction around the Sun-Galactic Center axis (each corona should share the small dipole in the direction of the motion of the disk in the halo). Note also that, although small, its angular shape and direction are known a priori, which facilitates a search for it. (iii) The signature of the asphericity of the halo depends on the unknown shape of the halo. On general grounds, one should expect a modulation of the emission in the angle,  $\psi$ , (as does the one treated in Sec. IV A), as well as a modulation in the azimuthal angle,  $\phi$  (as does the one treated in Sec. IV B which, however, should be smaller). Barring fine-tuned directions of the halo axes of symmetry, a more specific signature is an asymmetry pattern between the  $\psi, \phi$  and  $-\psi, \phi$  directions (reflection with respect to the Galactic plane), which cannot be mimicked by any of the two previously considered effects. Note that, although the relative magnitude of the anisotropy measured may change (whenever dark matter does not constitute a constant fraction to the diffuse gamma signal), the relative weights of the different Galactic asymmetries discussed here remain constant with energy. Since the diffuse radiation will be observed in many energy bands, one should keep in mind that the shape of this pattern must stay constant at each energy if it is to be attributed to dark matter. Also, if suspected dark matter spectral features appear, they should correlate with the amplitude of the angular asymmetries discussed in this paper. Combining angular and energy spectral information should surely strengthen our ability to distinguish dark matter annihilation radiation from other types of sources. Indeed, there is no a priori reason to expect that an astrophysical foreground affecting either the energy spectrum or the angular spectrum should appear in the other as well.

## VI. CONCLUSIONS

With the next generation satellite-based gamma ray telescope, GLAST, our measurements of the diffuse gamma ray spectrum will improve dramatically. Not only will the number of events observed increase, but also the spectrum will be studied up to considerably higher energies. Furthermore, much of the astrophysical contributions to the diffuse flux observed by EGRET will likely be resolved as point sources as a result of GLAST's superior angular resolution.

In this article, we have studied the signatures and distinctive features that would be possessed by dark matter annihilation radiation from either a dominantly Galactic or extragalactic population of dark matter. For an extragalactic contribution, we discussed the effect of observing dark matter radiation in a moving frame of reference (relative to the dark matter distribution), known as the Compton-Getting effect. We also discuss the ability to tie the angular distribution of annihilation radiation to the known structure of our (cosmologically speaking) local universe. This is especially interesting for gamma rays more energetic than  $\sim 100$  GeV, which can be absorbed by the cosmic infrared background radiation, effectively reducing the horizon for such particles.

If the diffuse dark matter annihilation radiation is instead dominated by the Galactic population, this flux will contain distinctive features resulting from the offset location and proper motion of the Solar System relative to the Galactic halo. Furthermore, any asphericity in the halo will have effects of the angular distribution of annihilation radiation. As in the extragalactic case, we also briefly discuss the anisotropies which are likely to result from inhomogeneities and substructure in the Galactic dark matter distribution.

GLAST's predecessor, EGRET, observed the presence of a diffuse gamma ray spectrum. Based on these observations, GLAST should see at least  $\sim 10^6$  photons per year. If a significant fraction of this flux is the product of dark matter, many of the angular features described here could potentially be identified. For example, if 10-15% of the diffuse flux observed by EGRET is dark matter annihilation radiation, in a decade of operations GLAST should be sensitive to anisotropies down to the level of 0.1%, well below the level required to study the angular signatures we have discussed in this paper.

### Acknowledgments

This work has been supported by the US Department of Energy and by NASA grant NAG5-10842.

### APPENDIX A: FLUX ENHANCEMENT DUE TO CLUMPINESS

Consider a cubic volume of size  $L$  at a distance  $D \gg L$  from us, such that the solid angle subtended by its surface is  $\Theta^2$ , where  $\Theta \equiv L/D$ . Let us assume that it is filled with: (i) a homogeneous distribution of dark matter with density  $\bar{\rho}$ ; (ii) a cubic dark matter clump of size  $l \ll L$  and density  $\rho_c$ , having the same mass (*i.e.*, such that  $\rho_c l^3 = \bar{\rho} L^3$ ). We denote with  $\bar{I}$  and  $I_c$  the differential photon fluxes (per area, per time, per solid angle) collected in the two cases, and with  $\bar{J} = \bar{I} \Theta^2$  and  $J_c = I_c \theta^2$  the flux per area per time, where  $\theta = l/D$ . If the angular resolution of our instrument is larger than  $\Theta$ , then the quantities  $\bar{J}$  and  $J_c$  are the relevant observables.

Let us assume now that  $I \propto \int_{\text{l.o.s.}} \rho^\kappa dx$ , where  $\kappa = 1$  corresponds to a decaying dark matter scenario and  $\kappa = 2$  to an annihilating dark matter one. One immediately sees that

$$I_c \propto \rho_c^\kappa l = \bar{\rho}^\kappa \left(\frac{L}{l}\right)^{3\kappa} l = \bar{\rho}^\kappa \left(\frac{L}{l}\right)^{3\kappa-1} L, \quad (\text{A1})$$

and

$$I_c = \bar{I} \left(\frac{L}{l}\right)^{3\kappa-1}, \quad (\text{A2})$$

from which it follows

$$J_c = \left(\frac{L}{l}\right)^{3\kappa-3} \bar{J} = \left(\frac{\rho_c}{\bar{\rho}}\right)^{\kappa-1} \bar{J}. \quad (\text{A3})$$

Equation (A3) implies that when  $\kappa = 1$  (the decaying dark matter scenario), only the angular information is sensitive to the clumpiness of the distribution. In other words, the total photon flux from decaying dark matter can be calculated (for a fixed particle physics scenario) once the profile of the *average* dark matter density is specified. This implies for example that the Galactic halo signal dominates over the cosmological one. For the  $\kappa = 2$  (annihilating dark matter) scenario, however, the picture changes considerably. In particular, the clumpiness of the dark matter distribution strongly effects both the angular distribution of the emission and the overall flux.

- 
- [1] V. Berezhinsky, A. Bottino and G. Mignola, Phys. Lett. B **325**, 136 (1994) [hep-ph/9402215]; A. Cesarini, F. Fucito, A. Lionetto, A. Morselli and P. Ullio, Astropart. Phys. **21**, 267 (2004) [astro-ph/0305075]; L. Bergstrom, P. Ullio and J. H. Buckley, Astropart. Phys. **9**, 137 (1998) [astro-ph/9712318]; D. Hooper and B. L. Dingus, Phys. Rev. D **70**, 113007 (2004) [astro-ph/0210617].
  - [2] N. W. Evans, F. Ferrer and S. Sarkar, Phys. Rev. D **69**, 123501 (2004) [astro-ph/0311145]; L. Bergstrom and D. Hooper, hep-ph/0512317; S. Profumo and M. Kamionkowski, astro-ph/0601249.
  - [3] X. J. Bi, Nucl. Phys. B **741**, 83 (2006) [astro-ph/0510714]; L. Pieri, E. Branchini and S. Hofmann, Phys. Rev. Lett. **95**, 211301 (2005) [astro-ph/0505356].
  - [4] J. F. Navarro *et al.*, Astrophys. J. **462** 563 (1996).
  - [5] B. Moore *et al.*, Phys. Rev. D **64** 063508 (2001).
  - [6] D. Merritt, S. Harfst and G. Bertone, [astro-ph/0610425]; G. Bertone and D. Merritt, Mod. Phys. Lett. A **20**, 1021 (2005) [astro-ph/0504422]; G. Bertone and D. Merritt, Phys. Rev. D **72**, 103502 (2005) [astro-ph/0501555]; Y. Mambrini, C. Munoz, E. Nezri and F. Prada, JCAP **0601**, 010 (2006) [hep-ph/0506204]; F. Prada, A. Klypin, J. Flix, M. Martinez and E. Simonneau, astro-ph/0401512; P. Ullio, H. Zhao and M. Kamionkowski, Phys. Rev. D **64**, 043504 (2001) [astro-ph/0101481]; G. Bertone, G. Sigl and J. Silk, Mon. Not. Roy. Astron. Soc. **337**, 98 (2002) [astro-ph/0203488]; P. Gondolo and J. Silk, Phys. Rev. Lett. **83**, 1719 (1999) [astro-ph/9906391].
  - [7] F. Aharonian *et al.* [The HESS Collaboration], Astron. Astrophys. **425**, L13 (2004) [astro-ph/0408145]; J. Albert *et al.* [MAGIC Collaboration], Astrophys. J. **638**, L101 (2006) [astro-ph/0512469]; K. Kosack *et al.* [The VERITAS Collaboration], Astrophys. J. **608**, L97 (2004) [astro-ph/0403422].
  - [8] G. Zaharijas and D. Hooper, Phys. Rev. D **73**, 103501 (2006) [astro-ph/0603540].

- [9] L. Bergstrom, J. Edsjo, P. Gondolo and P. Ullio, Phys. Rev. D **59**, 043506 (1999) [astro-ph/9806072].
- [10] L. Bergstrom, J. Edsjo and P. Ullio, Phys. Rev. Lett. **87**, 251301 (2001) [astro-ph/0105048].
- [11] P. Ullio, L. Bergstrom, J. Edsjo and C. G. Lacey, Phys. Rev. D **66**, 123502 (2002) [astro-ph/0207125].
- [12] D. Elsaesser and K. Mannheim, Astropart. Phys. **22**, 65 (2004) [astro-ph/0405347].
- [13] J. Silk and A. Stebbins, Astrophys. J. **411**, 439 (1993).
- [14] E. A. Baltz, J. E. Taylor and L. L. Wai, astro-ph/0610731.
- [15] V. Berezhinsky, V. Dokuchaev and Y. Eroshenko, Phys. Rev. D **68**, 103003 (2003) [astro-ph/0301551].
- [16] R. W. Michie Mon. Not. R. Astron. Soc. 125 127 (1963).
- [17] H. Zhao, J. E. Taylor, J. Silk and D. Hooper, Astrophys. J. in press, astro-ph/0508215; astro-ph/0502049; V. Berezhinsky, V. Dokuchaev and Y. Eroshenko, Phys. Rev. D **73**, 063504 (2006) [astro-ph/0511494]. A. M. Green and S. P. Goodwin, astro-ph/0604142; T. Goerdt, O. Y. Gnedin, B. Moore, J. Diemand and J. Stadel, Mon. Not. Roy. Astron. Soc. **375**, 191 (2007) [astro-ph/0608495].
- [18] J. E. Taylor and J. Silk, Mon. Not. Roy. Astron. Soc. **339**, 505 (2003) [astro-ph/0207299].
- [19] D. Elsaesser and K. Mannheim, Phys. Rev. Lett. **94**, 171302 (2005) [astro-ph/0405235].
- [20] P. Sreekumar *et al.* [EGRET Collaboration], Astrophys. J. **494**, 523 (1998) [astro-ph/9709257].
- [21] A. W. Strong, I. V. Moskalenko and O. Reimer, Astrophys. J. **613**, 956 (2004) [astro-ph/0405441].
- [22] S. Ando, Phys. Rev. Lett. **94**, 171303 (2005) [astro-ph/0503006].
- [23] W. M. Yao *et al.* [Particle Data Group], J. Phys. G **33**, 1 (2006).
- [24] A. H. Compton and I. A. Getting, Phys. Rev. **47**, 817 (1935).
- [25] M. Kachelrieß and P. D. Serpico, Phys. Lett. B **640**, 225 (2006) [astro-ph/0605462].
- [26] S. Ando and E. Komatsu, Phys. Rev. D **73**, 023521 (2006) [astro-ph/0512217].
- [27] A. Cuoco, S. Hannestad, T. Haugbolle, G. Miele, P. D. Serpico and H. Tu, astro-ph/0612559.
- [28] F. Aharonian *et al.* [HEGRA Collaboration], Astro. & Astrophys. **403** (2003) 523A.
- [29] C. Calaneo-Roldan and B. Moore, Phys. Rev. D **62**, 123005 (2000) [astro-ph/0010056].
- [30] R. Aloisio, P. Blasi and A. V. Olinto, Astrophys. J. **601**, 47 (2004) [astro-ph/0206036].
- [31] V. Berezhinsky, V. Dokuchaev and Y. Eroshenko, astro-ph/0612733.
- [32] D. Lynden-Bell, Mon. Not. Roy. Astron. Soc. **136**, 101 (1967).
- [33] A. K. Drukier, K. Freese and D. N. Spergel, Phys. Rev. D **33**, 3495 (1986).
- [34] R. P. Olling and M. R. Merrifield, Mon. Not. Roy. Astron. Soc. **311**, 361 (2000) [astro-ph/9907353].
- [35] R. P. Olling and M. R. Merrifield, Mon. Not. Roy. Astron. Soc. **326**, 164 (2001) [astro-ph/0104465].
- [36] S. M. Koushiappas, Phys. Rev. Lett. **97**, 191301 (2006) [astro-ph/0606208].
- [37] N. W. Evans, F. Ferrer and S. Sarkar, Phys. Rev. D **67**, 103005 (2003) [astro-ph/0212533]; P. Blasi and R. K. Sheth, Phys. Lett. B **486**, 233 (2000) [astro-ph/0006316].
- [38] N. Gehrels and P. Michelson, Astropart. Phys. **11**, 277 (1999); S. Peirani, R. Mohayaee and J. A. de Freitas Pacheco, Phys. Rev. D **70**, 043503 (2004) [astro-ph/0401378]; Also, see the URL: <http://www-glast.slac.stanford.edu/>
- [39] <http://www.mpi-hd.mpg.de/hfm/HESS/HESS.html>
- [40] <http://www.magic.iac.es/>
- [41] <http://veritas.sao.arizona.edu/>
- [42] S. Ando, E. Komatsu, T. Narumoto and T. Totani, astro-ph/0612467.